

Combining Map Displays and 3D Visualizations for the Analysis of Scalar Data on Cerebral Aneurysm Surfaces

Mathias Neugebauer^{†1}, Rocco Gasteiger¹, Oliver Beuing², Volker Diehl³, Martin Skalej², Bernhard Preim¹

¹Department of Simulation and Graphics, University of Magdeburg, Germany

²Department of Neuroradiology, University Hospital Magdeburg, Germany

³MR- and PET/CT-Center Bremen, Germany

Abstract

Cerebral aneurysms result from a congenital or evolved weakness of stabilizing parts of the vessel wall and potentially lead to rupture and a life-threatening bleeding. Current medical research concentrates on the integration of blood flow simulation results for risk assessment of cerebral aneurysms. Scalar flow characteristics close to the aneurysm surface, such as wall shear stress, form an important part of the simulation results. Aneurysms exhibit variable surface shapes with only few landmarks. Therefore, the exploration and mental correlation of different surface regions is a difficult task. In this paper, we present an approach for the intuitive and interactive overview visualization of near wall flow data that is mapped onto the surface of a 3D model of a cerebral aneurysm. We combine a multi-perspective 2D projection map with a standard 3D visualization and present techniques to facilitate the correlation between a 3D model and a related 2D map. An informal evaluation with 4 experienced radiologists has shown that the map-based overview actually improves the surface exploration. Furthermore, different color schemes were discussed and, as a result, an appropriate color scheme for the visual analysis of the wall shear stress is presented.

Categories and Subject Descriptors (according to ACM CCS):

Computer Graphics [I.3.6]: Methodology and Techniques, Interaction Techniques—Computer Graphics [I.3.7]: Three-Dimensional Graphics and Realism, Color, Shading, Shadowing, and Texture—Computer Graphics [I.3.8]: Applications —

1. Introduction

For many treatment planning tasks it is essential to map scalar data on medical surface data. As an example, [ZKS*96] mapped bone thickness data on the human skull to understand bone defects. Even in case of this static information with the well-known landmarks of the skull, it is difficult to navigate to surface regions of interest and put obtained information into the context of already visited parts of the surface. In case of more complex data such as simulation results mapped on surfaces with few landmarks, the exploration is even more difficult. As an example, the lateral distribution of the shear stress at the wall of a cerebral aneurysm,

a widened portion of a cerebral vascular structure, should be analyzed for diagnosis and treatment decisions. Since they are resulting from vascular deformations, the surface configuration changes among different aneurysms, even if they are roughly convex shaped. An overview visualization that simultaneously depicts all surface data, reduces the mental effort of exploring variable data mapped on varying surfaces. Additionally, this kind of presentation eases the recognition of spatial relations of corresponding surface regions that are potentially not visible at the same time.

In this paper, we describe a general strategy for supporting the exploration of scalar data mapped on cerebral aneurysm surfaces. We restrict ourselves to visualizing static simulation results, although the developed concept is also capable of dealing with dynamic data. It is based on flattening,

[†] mathias@isg.cs.uni-magdeburg.de

where 3D surface data is projected to a map. Our approach is inspired by other medical overview techniques, such as colon and brain flattening as well as the more abstract bull's eye plot used in cardiology. As a specific field of application we consider the exploration of the wall shear stress (WSS) mapped on the aneurysm and its supplying vascular structures. The map (map space) display is combined with a 3D visualization (model space). The map forms the contextual overview, used for spatial analysis and navigation, whereas the 3D visualization represents the focus, upon which the visual interpretation of the scalar surface data mainly takes place. The map display and the 3D visualization are synchronized, providing a bidirectional link. Thus, the orientation of the 3D visualization is adapted, if a certain position in the 2D map is selected and dragged. Alternatively, the map adapts itself after changing the orientation. Due to special map layout, it is possible to intuitively drag interesting scalar surface data from the map space into the model space.

We discuss the map layout, the distortions that are produced by our mapping strategy, the color scheme, and supporting map tools. Informal evaluations with 4 board-certified radiologists indicate that the technique may be learned in a short period of time and indeed presents the relevant information in a more coherent way compared to conventional facilities.

2. Medical Background

Cerebral aneurysms result from a congenital or evolved weakness of stabilizing parts of the vessel wall. Their incidence is estimated at 1-6% of the population [WWH03]. Saccular aneurysms represent the most common type of cerebral aneurysms (90%). They often occur at bifurcations of the basal brain artery. Aneurysms diverging from a balloon-like shape are referred to as fusiform aneurysms, the less common type. Both types are convex vessel expansions, with broad variations according to complexity and regularity. Cerebral aneurysms bear a high risk of rupture, which leads to cerebral bleedings, with often fatal consequences for the patient (fatality rate up to 67%). Due to an increase of performed MR scans, the number of accidentally found aneurysms is rising. Since the treatment bears a certain risk for the patient, the risk posed by an aneurysm has to be carefully estimated [VMM05]. Morphological features convey relevant information for estimation of the wall condition. As an example, areas of high local curvature indicate a possible previously occurred bleeding.

However, aneurysms often rupture although morphologic criteria did not reveal an increased risk. To better support the decision-making process, current medical research aims at the creation of useful, additional information derived from fluid dynamic simulations of the intravascular blood flow [CCA*05]. Blood flow simulations, carried out on patient-specific aneurysm FEM meshes, are based on simplifications the discussion of which is beyond the scope of this paper.

In essence, blood flow exhibits non-Newtonian characteristics, is a pulsatile flow and causes an elastic deformation of the vessel wall. The resulting data is complex. Amongst others, near wall information form an important component, since the wall stability - stress ratio has a main impact on the risk of rupture. Therefore, medical researchers are interested in an integrated analysis of scalar and the aforementioned morphological indicators. Thus, a combination of a 3D visualization (morphology) and a 2D map (navigation, scalar overview) is adequate to support the diagnosis.

3. Related Work

The regional distribution and location of functional and morphological data is important in medical research and diagnosis. A common technique is the map representation of functional MRI (fMRI) data, displaying activation levels of certain surface-near brain regions. These maps represent patches, defined by cerebral areas, or the whole surface, normally mapped on spheres or circles [JHS*05]. To enhance data visibility, morphological features are intentionally reduced by conformal flattening. In contrast, colon flattening represents morphological features on the inner colon surface [HAK00]. A cylindrical projection is applied and distortions are reduced by adaptive angular sampling during the projection. In [ZHT05], more sophisticated approaches are used to flatten branching vessels. To gain a conformal and an area preserving mapping, error minimization / optimization approaches are utilized.

These approaches are based on specific assumptions with respect to the basic surface shape (e.g. vessel, colon - cylindrical) or use anatomical definitions to produce specialized maps (e.g. cerebral regions and hemispheres). Even if they can roughly be described as convex shaped, aneurysms offer a wide range of morphological configurations, mainly resulting from a different placement, number and size of adjacent vessels. Their individual variability exceeds the one of cerebral surfaces, while in return only a few anatomical definitions are given. We therefore need a general approach to generate maps. A survey of general parameterization approaches is given in [SPR06]. For all planar approaches, a constraint defines the border of the map. If a feature of interest is separated by this map border, it naturally will be represented on different parts of the map domain. In order to obtain an unseparated depiction of this feature, by shifting it (interactively) towards the map center, a new parameterization with altered border constraints is necessary. In order to preserve the shape of the map domain, we need to fix its boundary. Since a map with static borders always exhibits distortions when based on arbitrary surfaces, we do not aim at reducing them. Instead, we aim at a more comprehensible presentation by giving them a static, global layout. Additionally, real-time interaction cannot be guaranteed, if complex medical surfaces have to be continuously parameterized dur-

ing interaction. This led us to a projection based approach with reduced computational effort.

Our approach is derived from multi-perspective views, which can be implemented in current graphics hardware at interactive rates [HWS*06]. The basic idea is to alter the projective image generation process in order to integrate multiple views into one viewport. A non-medical but nonetheless very inspiring application of multi-perspective views is described in [LTJ*08]. They smoothly integrate the bird's eye and the horizon perspective into one viewport to create an overview visualization of 3D city maps. The introduced cylinder-like distortions can be easily interpreted by the user. The viewport can be separated into three areas: the bird's eye, which can be described as focus, a transition zone, and the horizon view, which forms the context information. Our approach uses a related design in terms of distortions and focus-context-transition zones. To simplify the spatial correlation between map and model, we divide our multi-perspective map into zones, according to the associated viewports. This is inspired by the bull's eye plot [OGH*06], where different zones depict the diffusion of different myocardial sections. The bull's eye plot is based on standardized anatomical definitions, therefore its static layout is adequate. Aneurysms bear a high anatomical variability, thus a static layout is potentially suitable for only a small portion of all possible configurations. We therefore integrate a corresponding focus visualization that represents the underlying morphology as a colored 3D model and provide interactive mechanisms to dynamically alter the mapping by transferring features from map to focus and vice versa.

4. Visual Analysis of Cerebral Blood Flow in Aneurysms

With the development of an overview presentation of scalar simulation results near the aneurysm wall, we focus on one aspect of a pipeline for visual analysis of flow characteristics in cerebral aneurysms (see Fig. 1). This pipeline consists of several processing tasks, which eventually lead to the surface model and the simulation results that form the basis of our approach.

4.1. Visual Analysis Pipeline Overview

Since the analysis of flow dynamics mainly concentrates on unruptured aneurysms, we normally get MRA results as input image data. Depending on the clinical workflow and patient-specific circumstances (e.g. contrast agent compatibility), the vessels are contrast enhanced by usage of contrast agents or special MR sequences (e.g. TOF - time of flight). The segmentation can be performed with thresholding and requires only few manual corrective actions in most cases. The subsequent surface extraction is based on marching cubes. The resulting meshes are suitable for surface visualization, but not for simulation in terms of surface ele-

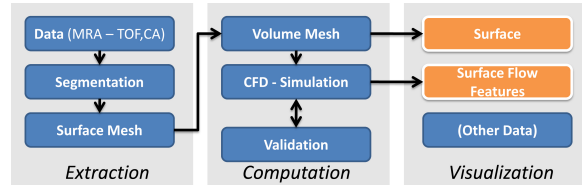


Figure 1: Pipeline for visual analysis of aneurysm flow features. The orange fields cover the application area of our approach.

ment quality (e.g. triangle aspect ratio). Therefore, a remeshing is applied [NJZ*08]. The resulting high quality surfaces are used to create FEM volume meshes on which the simulation is performed. In order to resemble realistic flow dynamics, the model assumption needs to be validated experimentally [JSB*07]. Our approach concentrates on simulation data near to the aneurysm wall, since it can be directly linked to the risk of rupture. We aim at giving an overview that enables the user to efficiently interpret the global data and navigate to local points of interest. Nevertheless, other simulation results, like internal flow features (e.g. vortices), are also important and require different visualization techniques.

4.2. Motivation and Requirements for Interactive Combined Map-Model Visualizations

Our goal is to present scalar surface data, such that relevant surface regions of interest are efficiently located and basic spatial relations between different surface parts can be identified. The exclusive presentation of a 3D model is not sufficient, since important information can be occluded. Depending on the complexity of the surface, a series of manual rotations can be necessary to gain a complete overview. This is associated with a high mental effort. In case of time-dependent data, it is almost impossible, since the rotation process itself needs a certain amount of time. Multiple viewports can reduce this problem, but it is still difficult to mentally combine these multiple images. Our approach aims at reducing this mental effort by smoothly arranging a multiple viewport overview around the 3D model with respect to spatial relations. Therefore, multiple viewports are combined into one 2D map. Detailed reasons for this decision and the consequential interaction and layout requirements are discussed in the following.

Combining Map and 3D Model: A 2D map delivers an instant overview of all surface data and makes it easy to find features of interest. If the map follows certain layout rules, it is also possible to spatially connect different surface regions (e.g. "A is opposite to B") that are not simultaneously visible in 3D. Nevertheless, morphological hints are reduced or lost and a 2D presentation introduces distortions, which can bias the visual analysis. Therefore, we apply a combined display:

the map M' forms the context, depicting all surface regions that are potentially not visible on the 3D model M . This model is the focus of our visualization whereon the analysis, aided by the information that can be retrieved from M' , takes place.

Correlation between Map and Model: To avoid redundancy, the map should only depict surface parts in M that are pointing away from the observer and thus are potentially occluded. The transition of a point from M' to M leads to a change of orientation of M . Subsequently, the point becomes visible on the surface and should not be visible on the map anymore. Beside this direct link of transition and rotation, additional correlation tools should be provided to mark points in M' and M simultaneously.

Interactive Map Manipulation: The map border forms a critical region, since a single surface region can be represented redundantly in the map domain when separated by the border (e.g., Fig. 2(C)). Due to this potential visual distraction, it should be possible to move a feature of interest away from the critical border area. As described above, this leads to a changed orientation of M . It becomes clear that interactive map manipulation forms the basis for transferring a point from M' to M and making it accessible for detailed analysis. This transition should lead to a comprehensible orientation change of M (e.g. translate map location leftwards, M rotates leftwards). Features in M' and M should be orientated similarly.

Map Distortion: The interactivity of the map manipulation is crucial for usability and the map is mainly used as contextual overview and for navigation support. Thus, a fast non-conformal map generation is suitable, as long as the introduced distortions bear a comprehensible layout. For an adequate transition of points from M' to M , the distortion should be low at map regions near to M .

Map Layout: The arrangement of M' relative to M must convey the spatial relations of surface regions with respect to their representations in the map domain. It should also be possible to spatially correlate these representations, since their simultaneous depiction is a main advantage of M' .

Color Map: For the final interpretation of the scalar values, the applied color map is essential. Due to the high spatial frequency of the WSS data, perceptual color maps, like the Heated Object Color Map, bear adequate characteristics in terms of depicting gradual scalar changes. It has to be discussed with users, which of the possible Color Maps is actually appropriate, since this strongly depends on special application requirements.

5. Overview Map: Creation, Layout and Characteristics

Due to the requirements (recall Sect. 4.2), we decided to apply a cube-map-based approach. The cube described in the following is not visible; it is used to clarify the projection

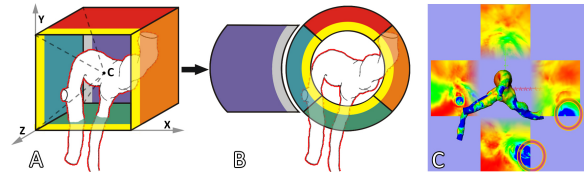


Figure 2: A: Cube Map: an axis-aligned cube is positioned at the center C of the aneurysm and the aneurysm's surface is projected onto five cube sides (dotted lines). B: The map zones created from the cube sides (color-coded to clarify the orientation coherence). C: Redundant feature depiction at cube borders.

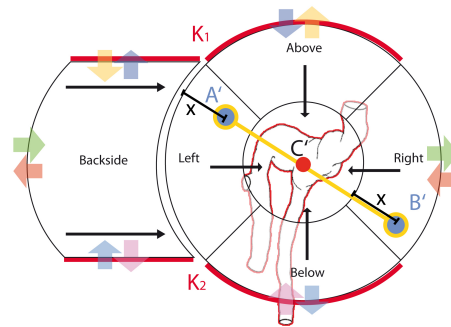


Figure 3: Map Layout: Colored arrows depict transitions between map borders. Black arrows show the transition paths towards the focus area (C'). Surface point A lies opposite to point B . Their map locations exhibit a linear coherence: $A'-C'-B'$.

process. Fig. 2(A) presents the cube map setup. The cube orientation is static to generate a direct link between regions depicted in the map and the orientation of the model. The observer's viewing direction is fixed towards the cube's front. To center the model within the cube, we utilize the model's center of gravity $C = (ec + bc)/2$, where ec is the Euclidean center with respect to wall distance and bc is the center of the oriented bounding box.

Starting from C , the model surface is projected onto each cube side, applying a perspective projection (45° viewing angle, 1:1 aspect ratio). The cube side pointing towards the observer is excluded from the whole projection process, since the related information is presented by the 3D model M . The resulting projected views are used to create the different map zones of M' (see Fig. 2(B)). They are part of our map layout (see Fig. 3) that satisfies the aforementioned requirements and bears the following features and characteristics:

Map Zones: A main part of the map forms a ring around the focus area containing the 3D model. Each quarter (in the following named L-(left), R-(right), A-(above), and B-(below) zone) of the ring is positioned close to the corre-

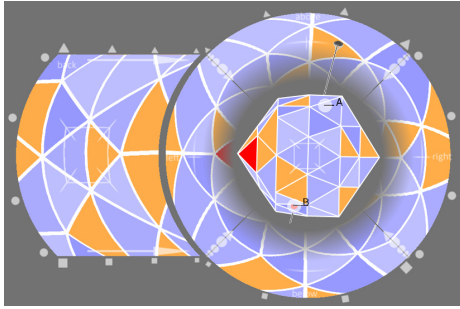


Figure 4: Distortion: An icosahedron is used to visualize the non-conformal, spherical distortion of the map.

sponding cube side. Since these cube sides point away from the observer, the map zones depict parts of the surface that are potentially not visible. The backside zone (BA-zone) is placed slightly remote on the left side. It forms an own focus area, inferior to the focus area containing the 3D model. Thus, we ease the visual correlation between front and back side. This correlation would be impossible, if the backside was also included into the ring layout, since a surface point lying opposite to the screen center of the 3D model would be represented as the outer edge of the ring, which implies a massive spatial distortion. Altogether, we achieve that dorsal and therefore most inaccessible surface parts are most distant to the focus area M , except for one unavoidable but non-serious case: the left half of the BA-zone. Respectively, surface points that are almost visible for the observer are close to the focus area.

Distortions: Since the quadric cube map sides are formed into ring quarters, we introduce non-conformal spherical distortions (see Fig. 4), mainly influenced by the ring width d . The overall distortion can be quantified by $c = \frac{1}{2}\pi * d$, where c describes the change of length of a surface line segment, if it is consecutively projected onto the inner and outer circle of the ring. To reduce the amount of distortion close to the focus area, we chose a ring width d that equals the length of the inner circle segment s (see Fig. 5). The non-ring layout of the BA-zone limits the maximum magnification of the features depicted in the map domain, due to the equal length of its inner and outer circle segments.

Cut Edges: An unfolded cube map bears incomprehensible cut edges, leading to 90° orientation changes during interaction (see Fig. 2). As an example, if a feature leaves the map leftwards, it appears from the top at the corresponding border. The ring layout reduces the number of these edges and permits a seamless transition of features from one ring zone to another. The likewise circular shape of the BA-zone provides the same for a transition towards/from the L-zone. The only exception are the cut edges K_1 and K_2 (see Fig. 3) resulting from the specialized design of the BA-zone. They bear an ascending change of orientation concerning the tran-

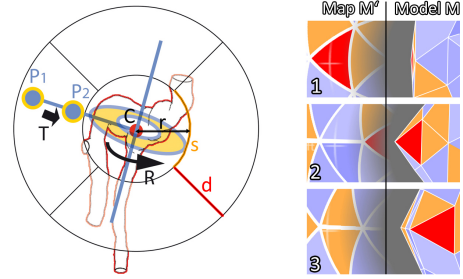


Figure 5: Interaction: The chosen path to translate (T) a map feature results into a comprehensible aligned rotation (R) of the model. **Right:** An example for the interactive transition of a feature (red triangle) from map to model. A similar feature orientation on map and model can be observed.

sition towards the A-/B-zone. This orientation change ranges from 90° to 225° . Due to the overall aspect ratio of the map, a vertical interaction scheme is aided. Since the extreme cut edges only occur at the upper and lower part, it is less distracting than the aforementioned disadvantages given by a ring layout of the BA-zone. Thus, we shift the unavoidable problem of cutting edge orientation change during interaction towards a map area that is likely outside the viewer's focus of attention.

Projection Artifacts: Since we apply a projection to create the map at interactive rates, it contains perspective artifacts. Due to the optimized placement of the projection center C , they play a small part in the overall distortion in most cases. They only become clearly noticeable, when "looking" inside a vessel (see Fig. 8, right). Since the map is used to analyze and correlate points on the aneurysm surface, these artifacts do not disturb the exploration process and can actually be seen as additional landmarks.

Interaction: The main interaction is transferring points from map to model by picking and dragging them towards the focus area (see Fig. 5). The underlying cube is static, so every transition of a map location equals a rotation of the model M and vice versa. The combination of the unfolded cube and the projection from within the model M (see Fig. 2(A)) leads to desired effects during interaction: A leftwards translation of a map point leads to a leftwards rotation of the model and the corresponding surface point appears at the right side of the model. It has the same orientation as the map point. These observations are true for all transitions towards the screen center of the focus.

Inter-Map Correlation: Since it is derived from a cube, the inner ring layout roughly depicts opposing surface regions (A-zone / B-zone; L-zone / R-zone). It also contains detailed, surface point-wise correlations. We define two surface points A and B as opposing, if they are collinear with the aneurysm center C . Depending on the ring width d , the map



Figure 6: Data for Correlation Tool: The surface colors of the model (A) encode world coordinates used to link them with map coordinates (B).

point A' is opposed to $B' = C' + \left(\frac{\overrightarrow{A'C'}}{\|\overrightarrow{A'C'}\|} \right) * (r + x)$, whereas C' is the screen center of the ring, r the inner radius and x the distance to the inner/outer ring border of A/B (see Fig. 3, Fig. 5). Thus, two opposing points exhibit a static distance. The correlation tool described in Section 6 utilizes this linear and intuitive relation, resulting from our map layout.

6. Implementation Details

To obtain the map, five additional rendering passes for each frame are performed, resulting in five offscreen images, one for each cube side. The perspective camera is positioned at C and transformed according to the cube side that is represented by the current rendering pass. The scalar values encoded at each vertex position are mapped to a color. Lighting is disabled to avoid visible intensity seams in the final map. The resulting image is rendered offscreen into a texture (512×512), utilizing OpenGL's render-to-texture functionalities. The texture resolution is sufficient for standard screen resolutions ($\leq 1280 * 1024$) since the map zones cover only a small portion of the screen space. The map zones are formed by quadstrips. To avoid linear interpolation artifacts when the textures are applied, each map zone consists of 64 segments, providing the texture coordinates. We want to link positions on the map with positions on the model surface (necessary for the correlation tool). Thus, we apply a second 5-pass rendering, but this time the world coordinates are encoded by colors on the surface. The color coding is carried out per vertex, utilizing a GLSL shader that maps the (x, y, z) position relative to the bounding box on the (r, g, b) color of the vertex. These additional textures are evaluated during the usage of the correlation tool.

Correlation Tool: By clicking on the map, this tool marks the selected map point and its opposing map point, as well as the corresponding locations on the surface (see Fig. 7). The opposing point is efficiently calculated from the aforementioned linear relation of map points on the inner ring. Both points are used as manually placed landmarks. By disabling the depth test during rendering, we make them permanently visible on the model surface. Different colors are employed to convey whether or not a point is occluded by the model.

Overlay: A pictogram-based overlay is utilized to support the map interaction. Arrows depict the transition paths

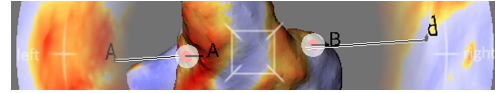


Figure 7: Correlation Tool: If a point A on the map is selected, it is marked on the map and the surface, as well as the opposite point B.

for dragging points towards the focus. Symbols are placed at the map borders to clarify border relations in terms of transition and orientation. The symbols correlate according to their size and shape. Two crosshairs support the visual link between the front (3D model) and backside (BA-zone) and illustrate the distortion and change of size in the BA-zone.

7. Results and Informal Evaluation

We applied our approach to datasets of the two standard types of cerebral aneurysms: a saccular (AN01: 30.946 Δ) and a fusiform aneurysm (AN02: 65.180 Δ). To create the surface and simulation data, we applied the pipeline described in Section 4.1. Despite the non-optimized, prototype software state, interactive frame rates (> 15 fps) can be achieved on a middle-class laptop (2Ghz Core Duo, 2GB Ram, 256 MB ATI HD 2600). The applied color map results from discussions with radiological experts.

Figures 8 and 9 depict examples of our overview approach. Figure 8 shows a continuous ring structure of increased wall shear stress. In stand-alone 3D model views, the continuous nature of this ring is hard to grasp, since it follows a complicated path that is occluded by several vessel inlets. The relationship between inlet and regions of increased wall shear stress on the opposing aneurysm wall can also be easily identified.

The overview visualization was presented to four radiologists (> 5 years working experience) who are familiar with slice and DVR based imaging of cerebral aneurysms. During the evaluation they were asked to select a surface region and describe the WSS distribution at the opposing aneurysm wall (with and without usage of the correlation tool) and navigate to these regions. They stated subjective ratings for certain aspects of the interaction (see Table 1) and also gave free statements as part of an interview. A direct comparison with existing techniques was not possible, since the analysis of scalar values mapped on surface models is not part of the current aneurysm diagnosis workflow.

Despite being unfamiliar with this kind of surface representation, all experts were able to accomplish the given task. After a few minutes they were able to freely navigate to surface features of interest. The information conveyed by the overlay was considered useful and not distracting from the underlying map. The correlation tool was frequently used to place landmarks and was appreciated. As a surprise, one expert (mainly dealing with slice-based imaging) was able to

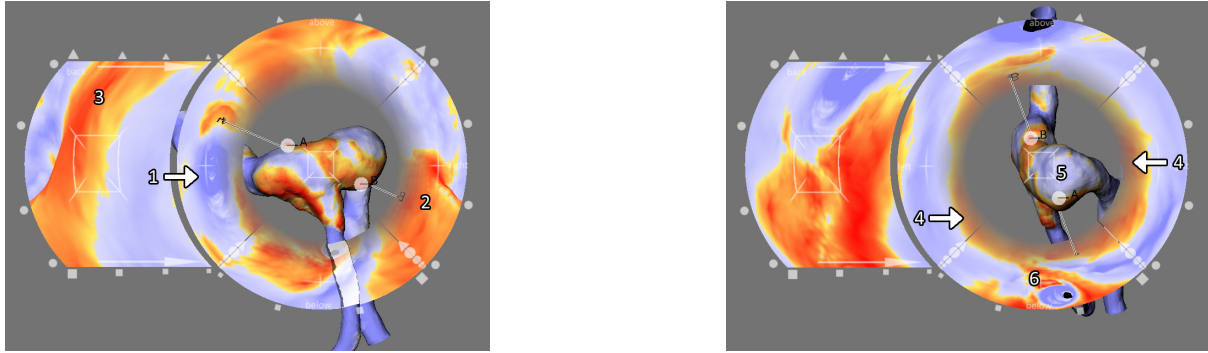


Figure 8: Fusiform Aneurysm AN02: *Left:* The relation between the area of higher WSS (2) and the opposing vessel inlet (1) becomes clearly visible, as well as the area of higher WSS at the back of the aneurysm (3) (not visible on the 3D model) *Right:* A closed ring of higher WSS (4) enclosing a low WSS area (5), and a projection artifact at the vessel inlet (6) can be observed.

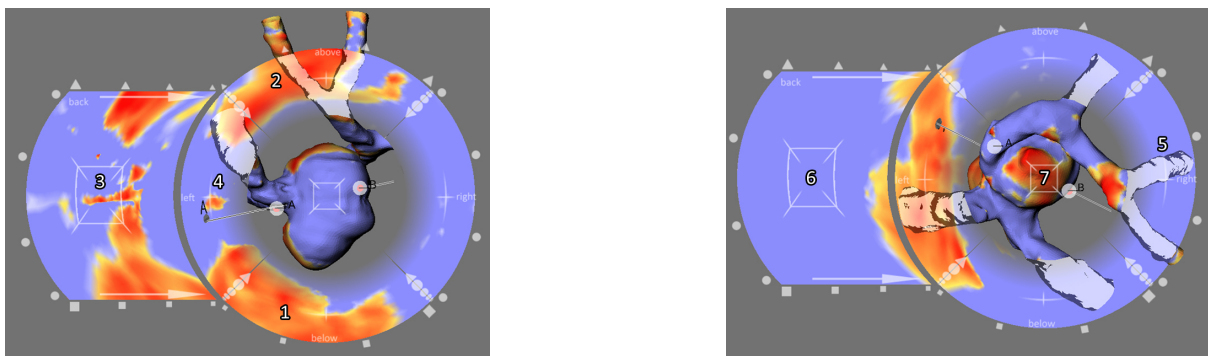


Figure 9: Saccular Aneurysm AN01: *Left:* Areas of high WSS at the lower (1) and upper (2) side of the aneurysm and a small, defined WSS feature at the backside (3). *Correlation Tool:* A landmark placed at a local area of higher WSS (4). The related point A and its opposing point B were marked. *Right:* Vessels that occlude the map are rendered in a semi-transparent, silhouette-enhancing toon style (5). Low WSS (6) at the backside, opposite to the area of higher WSS in the focus (7).

	Exp1	Exp2	Exp3	Exp4	θ
Learning Effort	2	1	2	3	2
Usability	2	2	3	2	2.25
Overview	2	1	2	2	1.75
Correlation (NT)	3	2	3	2	2.5
Correlation (T)	1	1	2	2	1.5

Table 1: The rating from 1 (good) to 5 (bad) of different characteristics: the effort to understand the visualization, the complexity of interaction, the overview and the correlation between map and model without (NT) and with (T) usage of the correlation tool.

correlate a projection artifact correctly with the according vessel inlet in the 3D model, without using the correlation tool. The distortion resulting from the ring layout of the map zones was considered as non-distracting, since it exhibits a global, spherical layout.

To define an adequate color map, we presented a preset of possible color maps to all experts. Our hypothesis was that a detailed depiction of scalar graduations as well as an overall classification in high and low values would be of interest. The scalar wall shear stress data has a high spatial frequency. According to [Lev97], we choose the following established color maps: Linear Grayscale Map (LG), Optimized Color Map (OC) and Heated Object Map (HO) (see Fig. 10). Although radiologists often work with grayscale images, the LG was rated the worst. The experts requested a colored map, as it is common in Doppler ultrasonography, where red and blue colors indicate blood flow directions. Although OC and HO were rated as good in terms of scalar value estimation, the lack of a more defined distinction between high and low values was criticized. As a consequence, we designed a Split Color Map with different color maps for high and low values. The threshold was defined manually during the evaluation. Combinations of OC, HC and LG in one Split Color Map were considered confusing, due to the high num-

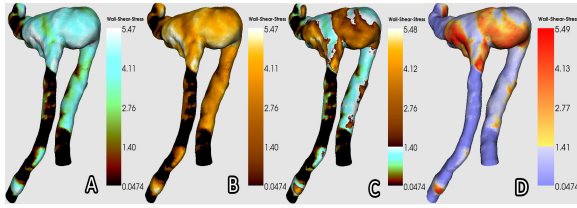


Figure 10: A selection of the color maps that were discussed in the evaluation: Optimized Color Map (A), Heated Object Color Map (B), both combined in a Split Color Map (C) and the color map that resulted from the discussion (D).

ber of different colors and similar colors for different scalars in some cases (see Fig. 10 C). To avoid this and still give a more binary representation while preserving the graduation, we applied two primary color maps. These perceptual maps present scalar graduation by linking it to the luminance of a color. According to the experts' input, the final color map was defined with the following characteristics: the low value range is colored from dark blue to light blue, the high value range from orange to red. Due to their complementary nature, the step from light blue to yellow is harmonic but still distinguishable. Red is an established signal color in medical applications.

8. Conclusion and Outlook

We described a combination of a map display with a 3D visualization of a cerebral aneurysm in order to give a complete overview on simulation results. Our map design focuses on a fast interactive exploration and on providing bidirectional links between information presented in the map and information mapped onto the aneurysm surface. Our discussion was focused on visualizing simulated wall shear stress data. However, our method is not restricted to the exploration of this specific data. Other simulation data near the aneurysm wall can be displayed as well.

The informal evaluation demonstrated that radiologists can use the combined visualization after 5-10 minutes effectively. After this learning period, radiologists consider the visualization as comprehensible and appreciate that they can get a useful overview for efficiently locating regions of interest. Both, the manipulation of the map and the manipulation of the model turned out to be useful to examine wall shear stress data. The informal evaluation revealed that the integrated display of curvature-based surface features would further enhance the usefulness, since areas of high local curvature indicate possible former bleedings.

Because information related to the whole surface is visible, we assume that our method leads to significant advantages, when dynamic data should be displayed on the surface. Moreover, we will evaluate and refine the map display for documentation purposes (e.g. printed Medical Records).

For such tasks, in particular, annotation is necessary. Finally, comparative visualization is an essential use case for our visualization technique, where the development of an aneurysm should be evaluated by means of simulation results at different points in time.

Acknowledgment: We would like to thank G. Janiga and S. Seshadri (ISUT Magdeburg) for providing the simulation data, U. Preim and her colleagues (University Hospital Magdeburg) for fruitful discussions and Fraunhofer MEVIS for providing the prototyping platform MeVisLab.

References

- [CCA*05] CEBRAL J., CASTRO M., APPANABOYINA S., ET AL.: Efficient pipeline for image-based patient-specific analysis of cerebral aneurysm hemodynamics: technique and sensitivity. *IEEE Trans. on Med. Im.* 24 (2005), 457–467.
- [HAK00] HAKER S., ANGENENT S., KIKINIS R.: Nondistorting flattening maps and the 3D visualization of colon CT images. *IEEE Trans. on Med. Im.* 19 (2000), 665–670.
- [HWS*06] HOU X., WEI L., SHUM B., ET AL.: Real-time multi-perspective rendering on graphics hardware. In *ACM SIGGRAPH 2006 Sketches* (2006).
- [JHS*05] JUA L., HURDALB M., STERN J., ET AL.: Quantitative evaluation of three cortical surface flattening methods. *NeuroImage* 28 (2005), 869 – 889.
- [JSB*07] JANIGA G., SESHADHRI S., BORDÁS R., ET AL.: Experimental Validation of CFD Results in the Model of an Artificial Aortic Aneurysm. In *ANSYS Conference* (2007), pp. paper 2.2.8, Presentation.
- [Lev97] LEVKOWITZ H.: *Color Theory and Modeling for Computer Graphics, Visualization, and Multimedia Applications*. Kluwer Academic Publishers, 1997.
- [LTJ*08] LORENZ H., TRAPP M., JOBST M., ET AL.: Interactive Multi-Perspective Views of Virtual 3D Landscape and City Models. In *Proc. of the 11th AGILE Int. Conf. on GI Science* (2008).
- [NJZ*08] NEUGEBAUER, JANIGA, ZACHOW, ET AL.: Generierung qualitativ hochwertiger Modelle fuer die Simulation von Blutfluss in zerebralen Aneurysmen. In *SimVis* (2008), pp. 221 – 236.
- [OGH*06] OELTZE S., GROTHUES F., HENNEMUTH A., ET AL.: Integrated Visualization of Morphologic and Perfusion Data for the Analysis of Coronary Artery Disease. In *Proc. of EuroVis* (2006), pp. 131–138.
- [SPR06] SHEFFER A., PRAUN E., ROSE K.: Mesh parameterization methods and their applications. *Found. Trends. Comput. Graph. Vis.* 2 (2006), 105–171.
- [VMM05] VINDLACHERUVU R., MENDELOW A., MITCHELL P.: Risk-benefit analysis of the treatment of unruptured intracranial aneurysms. *JNNP* 76 (2005), 234–239.
- [WWH03] WIEBERS D., WHISNANT J., HUSTON J.: Unruptured intracranial aneurysms: natural history, clinical outcome, and risks of surgical and endovascular treatment. *Lancet* 362 (2003), 103 – 110.
- [ZHT05] ZHU L., HAKER S., TANNENBAUM A.: Flattening maps for the visualization of multibranch vessels. *IEEE Trans. on Med. Im.* 24 (2005), 191–198.
- [ZKS*96] ZUIDERVELD K., KONING A., STOKKING R., ET AL.: Multimodality visualization of medical volume data. *Computers & Graphics* 20 (1996), 775–791.